Charge Transport Mechanism in K_2ZrO_3

Shivendu Tripathi
Department of physics, Satish Chandra College, Ballia, U.P. -277001

The electrical conductivities and thermoelectric power studies of potassium zirconate (K_2ZrO_3) have been investigated in this paper. The compound has been prepared in the laboratory by solid state reaction method. Ionic and electronic conductivities have also been calculated. Temperature dependence of thermoelectric power has been examined. Accordingly, paddle wheel mechanism has been found suitable to explain the ion transport mechanism in the alkali (K^+) metal zirconates.

Keywords: Electrical conductivity, Ionic conductivity, Electronic conductivity, Thermoelectric power, Phase Transition Temperature, Paddle wheel mechanism

1. INTRODUCTION

Superionic conductors constitute a particular class of solid materials characterised by ionic conductivity of an order of magnitude as is usually found in case of molten salts. The ionic conductivity exists due to the movement of one type of ions between sites provided by the immobile ion- sublattice, which is undergoing thermal vibrations about fixed equilibrium position. A large number of fast ion-conducting solids, namely with Ag^+, Cu^+, Li^+, Na^+, K^+, H^+, F^+, and O^{-2} ion conduction have been discovered in the last five decades [11-19]. Some of these alkali-based superionic conductors are of technological importance as solid electrolytes for all solid alkali batteries and may solve the safety problem of the rechargeable alkali ion batteries using non-aqueous liquid electrolytes. Further, alkali metal zirconates have been reported as good candidates of solid sorbents for CO, capture in terms of large CO_2 sorption capacity, infinite CO_2/N_2 or CO_2H_2 selectivity, good reversibility, and high operating temperature. The structural, electronic, and phonon properties of K_2ZrO_3 have been investigated by combining the density functional theory with lattice phonon dynamics [1-11].

Electrical conductivities and thermoelectric power have been studied in both, normal and superionic phases. Heats of transport, activation energy, and enthalpy of the compounds

2. MATERIAL PREPARATION AND EXPERIMENTAL TECHNIQUES

The specimen compound K_2ZrO_3 has been prepared in the laboratory by solid state reaction method. The starting materials for the preparation of K_2CO_3 and ZrO_2, have been used to prepare K_2ZrO_3. Reactants are taken in the ratio of their molecular weights and then thoroughly mixed. Afterword, the mixture is fired in the air in a silica crucible for 60 hours for preparing the K_2ZrO_3 at 1000K with one intermediate grinding. Reaction for the preparation of K_2ZrO_3 is shown as

$$K_2CO_3 + ZrO_2 \xrightarrow{1000K,60hrs} K_2ZrO_3 + CO_2$$

The characterization of these compounds has been done using X-rays diffraction data, which elucidated that the compound potassium zirconate has monoclinic structure.

Measurements of ac and de electrical conductivities of K_2ZrO_3 have been carried out as a function of various parameters such as frequency, time and temperature. Further, temperature dependent thermoelectric power studies of the samples have been performed.

3. ELECTRICAL CONDUCTIVITY MEASUREMENT

An ac signal of small strength is applied on the sample during the measurement of its electrical conductivity. The obtained conductivity is referred to as *ac* electrical conductivity, $\sigma_{ac}(\omega)$. The *ac* conductivity becomes a function of the applied signal frequency if the sample has some sort of dipoles of higher relaxation time or grain boundary or space charge concentration in it. When the sample is subjected to the *dc* signal, the measured conductivity is referred to as *dc* electrical conductivity, σ_{dc}. Most of the methods used for the measurement of $\sigma_{ac}(\omega)$can also be used for the measurement of σ_{dc}. However, in case of mixed conduction (ionic plus electronic conduction), several complexities are encountered while measuring σ_{dc} because the effective field is reduced by blocking of ionic charge at the electrodes; so it becomes time dependent. Due to this reason, it is often convenient to record instantaneous current through and voltage across the sample. Tentatively, all measurements need certain time, hence instantaneous current cannot be recorded. Therefore, current through the sample is recorded as the function of time and a small extrapolation of the curve on the lower side gives instantaneous current. At t = 0, σ_{dc} becomes less than σ_{ac} if grain boundary or air pores are present in the material of the sample. An ac signal of small strength is applied on the sample during the measurement of its electrical conductivity. The obtained conductivity is referred to as *ac* electrical conductivity, $\sigma_{ac}(\omega)$. The *ac* conductivity becomes a function of the applied signal frequency if the sample has some sort of dipoles of higher relaxation time or grain boundary or space charge concentration in it. When the sample is subjected to the *dc* signal, the measured conductivity is referred to as *dc* electrical conductivity, σ_{dc}. Most of the methods used for the measurement of $\sigma_{ac}(\omega)$can also be used for the measurement of σ_{dc}. However, in case of mixed conduction (ionic plus electronic conduction), several complexities are encountered while measuring σ_{dc} because the effective field is reduced by blocking of ionic charge at the electrodes; so it becomes time dependent. Due to this reason, it is often convenient to record instantaneous current through and voltage across the sample. Tentatively, all measurements need certain time, hence instantaneous current cannot be recorded. Therefore, current through the sample is recorded as the function of time and a small extrapolation of the curve on the lower side gives instantaneous current. At t = 0, σ_{dc} becomes less than σ_{ac} if grain boundary or air pores are present in the material of the sample.

3.1. Electrical Conductivity as a Function of Frequency

The electrical conductivity, σ of K_2ZrO_3 has been measured at few fixed frequencies. Results are shown in Figure 1. As evident from Figure 1, there is no difference between σ_{dc} (0) and σ_{ac} values. Also there appears no appreciable difference among the σ values at different frequencies. These results indicate that grain boundary effects are minimised and no pore exists in the samples.

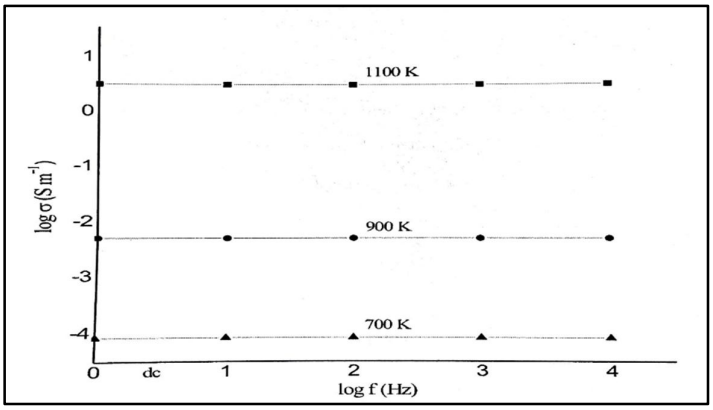

Fig. 1: Plot of logarithm of conductivity (log σ) vs logarithm of frequency (log f).

3.2. Electrical Conductivity as a Function of Time

Typical plots of time dependent study of electrical conductivity (σ) at low but constant electric field carried out on the samples, are shown in Fig. 2. Graphical representation at only three temperatures have been shown in Fig. 2 because at other temperatures, these plots exhibit similar nature.

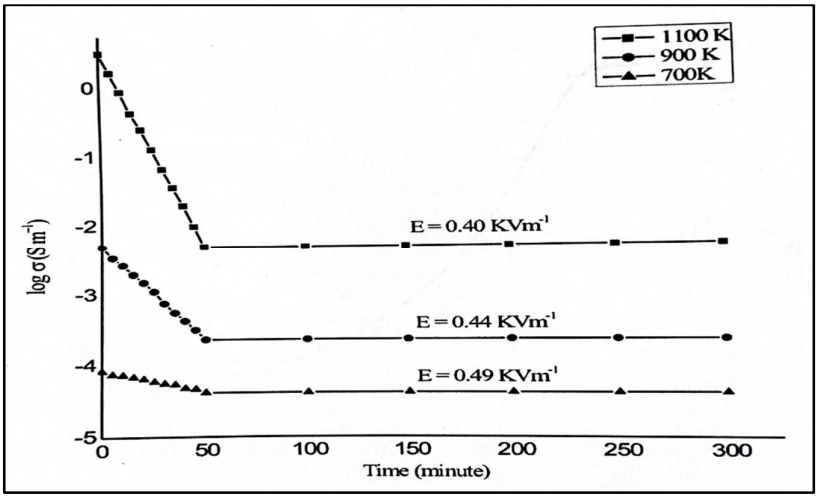

Fig. 2: Plot of logarithm of conductivity (log σ) vs time.

In general, σ decreases with time and tends to become constant. The trend of constancy starts appearing after a short interval of time at lower temperatures but increases with increasing temperature. This decrease in σ with time occurs due to the blocking of ions at the electrodes. Obviously, the constant value of σ_{dc} after a long time ($t \rightarrow \infty$), is the electronic part (σ_e) of the conductivity and the value of σ_{dc} for $t \rightarrow 0$ is the total (ionic + electronic) conductivity. In time dependent study, σ_{dc} (0) and σ_{dc} (∞) have been obtained at each temperature. The ratio of ionic to electronic conductivity ($r = \sigma_i / \sigma_e$) has been calculated using the following relations

$$r = \frac{\sigma_i}{\sigma_e} = \frac{\sigma - \sigma_e}{\sigma_e}$$
$$r = \frac{\sigma_{dc}(t \rightarrow 0) - \sigma_{dc}(t \rightarrow \infty)}{\sigma_{dc}(t \rightarrow \infty)} \quad (1)$$

$$\sigma_i = \left(\frac{r}{r+1}\right)\sigma$$
$$\sigma_e = \left(\frac{1}{r+1}\right)\sigma \quad (2)$$

Temperature dependence of log(r) has been shown in Figure 3. The contribution of ionic and electronic conductivities to the total conductivity at various temperatures has been shown in Figure 3 by using the equation (2).

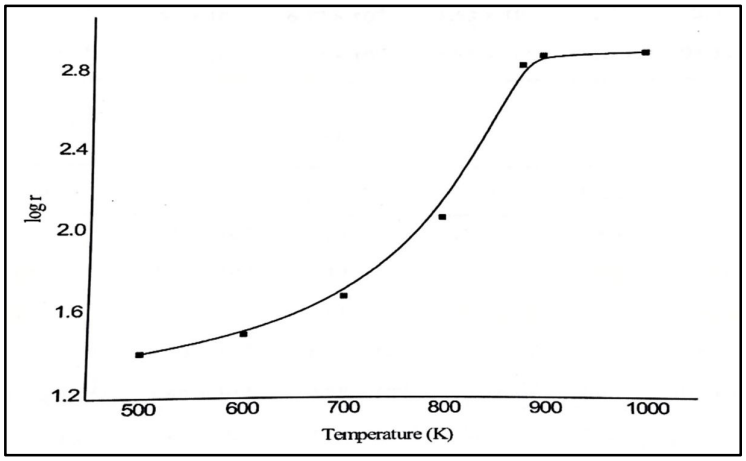

Fig. 3: Plot of log r vs temperature.

The calculated values of the ratio of ionic to electronic conductivity ($r = \sigma_i / \sigma_e$), ionic conductivity (σ_i) and electronic conductivity (σ_e) have been given in Table 1.

Table 1: Total conductivity (σ), ionic conductivity (σ_i), electronic conductivity (σ_e), ratio of ionic to electronic conductivity (r) and percentage contribution of ionic conductivity at different temperatures.

T(K)	σ (Sm^{-1})	σ_e (Sm^{-1})	σ_i (Sm^{-1})	r	log r	% of σ_i
1100	3.24	5.12×10^{-3}	3.23	6.31×10^{2}	2.80	99.84
1000	2.18	4.21×10^{-3}	2.17	5.16×10^{2}	2.71	99.80
980	1.02	3.21×10^{-3}	1.01	3.16×10^{2}	2.50	99.68
900	5.08×10^{-3}	2.34×10^{-4}	4.85×10^{-3}	2.07×10^{1}	1.31	95.31
800	1.12×10^{-4}	1.50×10^{-5}	9.70×10^{-5}	6.46×10^{1}	0.81	86.60
700	8.34×10^{-5}	4.12×10^{-6}	7.92×10^{-5}	1.92×10^{1}	1.28	95.05
600	5.24×10^{-6}	4.36×10^{-7}	4.08×10^{-6}	1.10×10^{1}	1.04	91.67
500	1.17×10^{-7}	1.00×10^{-8}	1.07×10^{-7}	1.10×10^{1}	1.02	91.45

As evident from Table 1, ionic contribution to total electrical conductivity increases with temperature but remains less than 95% for K_2ZrO_3, below a particular temperature. Above this particular temperature, the ionic contribution suddenly increases and becomes more than 99% for the compound. This clearly indicates that the solid possess two phases: one phase below and the other above the particular temperature. The particular temperature, at which a demarcation between the two phases occurs, is termed as phase transition temperature (T_p). Further, electronic conductivity also increases with temperature although it remains very weak (~10^{-4} Sm^{-1}).

3.3. Electrical Conductivity as a Function of Temperature

The electrical conductivity of K_2ZrO_3, has been measured as a function of temperature during both heating and cooling cycles. Results are shown in Fig. 4 as log σT vs T^{-1} plots, which can be divided into three regions: (i) a linear region below the certain temperature ($T<T_1$), (ii) a non- linear region between T_1 and T_2 ($T_1<T<T_2$), and (iii) a flat and linear region above the certain temperature ($T> T_2$). In the linear region ($T<T_1$), the electrical conductivity is predominantly due to ionic conduction with 2 to 7% electronic contribution 5 to 9% for K_2ZrO_3. This region exhibits mixed conduction which is normal ionic phase of the compound. The linear region can be expressed by the equation as,

$$\sigma_i T = \sigma_0 \exp^{\frac{-E_a}{kT}} \quad (3)$$

In flat and linear region above T_2 the electrical conductivity is entirely due to the jons with almost negligible electronic contribution. The value of σ_i is found to be high (3.23 Sm^{-1} for K_2ZrO_3) in this region which comes in the range of superionic phase. Thus, the compound K_2ZrO_3 pass into the superionic phase above T_p and normal ionic phase below T_p.

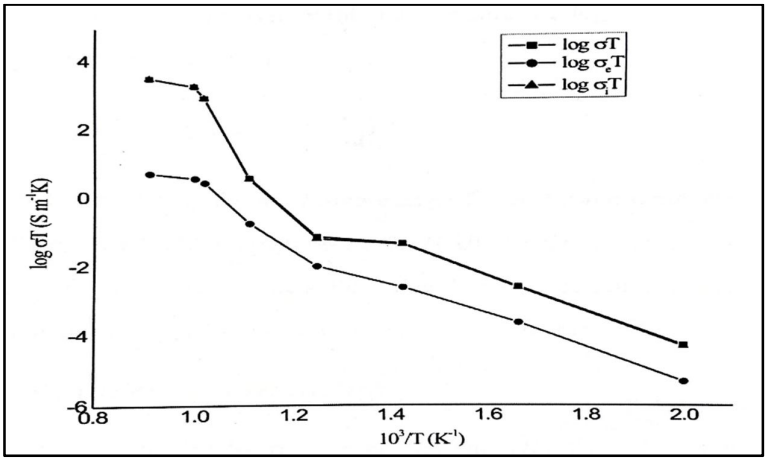

Fig. 4: Plot of logarithm of conductivity & temperature (log σT) vs inverse of temperature T^{-1}.

Further, the log $\sigma_e T$ vs T^{-1} plot is almost similar in nature as compared to log σT vs T^{-1} plots. The ionic conductivity (σ_i) increases by several orders of magnitude at the same temperature at which total electrical conductivity (σ) jumps; but in the superionic phase of the solids the values of σ_e are found to be very small in comparison to σ, which indicates that there occurs a structural change in the solid at the phase transition temperature. Below this temperature the log σT vs T^{-1} plot is linear and expressed by the equation,

$$\sigma_e T = \sigma_0 \exp^{\frac{-\omega}{kT}} \tag{4}$$

where σ_0 is constant and ω is the activation energy for electronic conduction. The value of σ (0.66 eV for K_2ZrO_3) is large but not enough to relate it to the energy band gap of the solids. The electronic conduction occurs due to hopping of electrons trapped at the defect centres present in the solids.

4. Thermoelectric Power Measurement

The results of thermoelectric power (S) measurement are graphically presented in the form of S vs T^{-1} plot as shown in the Fig. 5. This plot can be divided into three regions: (i) a linear region below T_1($T < T_1$), (ii) a nonlinear region between T_1 and T_2 ($T_1 < T < T_2$) and (iii) a linear region above T_2 ($T > T_2$) In the linear region, S can be expressed as

$$S = \frac{Q}{eT} + H \tag{5}$$

Using Equation 5, values of Q and H are calculated from the linear portion of the plots shown in Figure 5.

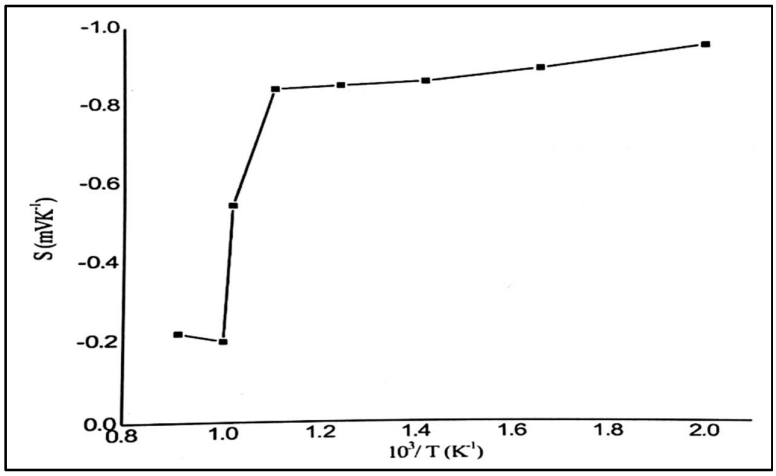

Fig. 5: Plot of Thermoelectric power (*S*) vs inverse of temperature T^{-1}.

Further, the linear region of plots log σT vs T^{-1} (Fig. 4) has been used to evaluate the values of enthalpy for ion migration h_m and temperature independent constant C_2. The values of E_a, C_2, Q, H and S are given in Table 2.

Table 2: Summarised result of activation energy (E_a), C, heat of transport (Q), H and thermoelectric power (*S*).

Temperature	**E_a = h_m (eV)**	**C = σ_0 (Sm^{-1})**	**Q (eV)**	**H (mVK^{-1})**	***S*** **(mVK^{-1}) at 1100 K**
High temperature region ($T>T_2$) K	0.39	1.95×10^5	0.67	-0.46	-0.88
Low temperature region ($T<T_1$) K	1.94	5.51×10^6	0.15	-0.62	
Here T_1 = 970 K, T_2 = 990 K and T_p = 980 K					

5. DISCUSSION

Thermoelectric power is accompanied with a negative sign throughout the temperature range. This indicates that the entity of charge carriers in K_2ZrO_3 is positive in nature. There are two types of positively charged ions namely, K^+ and Zr^{+3} ions in K_2ZrO_3. The Zr^{+3} ions have high positive charge and also bigger ionic size in comparison to K^+ ions. Therefore, it is least probable that Zr^{+3} ions are mobile in the solids. Instead, K^+ ions are expected to possess higher mobility due to their lower positive charge and smaller ionic size as compared to Zr^{+3} ions. The general transport mechanism of such ions is hopping. However, intrinsic hopping conduction of these ions from normal lattice site to other lattice site is least probable because it will involve high activation energy (-5 eV or more). Hence electrical conduction may be attributed to the hopping of defects. In view of the fact that a perfect ionic crystal behaves like an insulator, point defects (Frenkel or Schottky) are necessary for ion transport in such solids.

Due to thermal vibrations, ions sometimes receive energy enough to be pushed into an interstitial site or to a nearby vacant lattice site. This leads to an ionic conduction when an electric field gradient is set up across the sample. The value of S is high which indicates that only one type of charge carrier is responsible for electrical conduction. As observed by thermoelectric power studies, the nature of charge carriers is positive. Therefore, it appears that there exists a large number of Frenkel defects even in normal ionic phase of the sample, which may further be generated at higher temperatures. At low temperatures i.e. in normal ionic phase, thermal generation of appreciable number of Frenkel defects is less probable because high energy is involved in their generation. Thus, the number of thermally generated Frenkel defects remains essentially constant below the phase transition temperature. In such a situation, the slope appearing in the linear portion of log σT vs T^{-1} plots (Fig. 4) below the phase transition temperature gives the activation energy (E_a); which is actually the enthalpy for the migration of mobile defects (h_m). The value of h_m comes out to be of the order of 0.39 eV for K_2ZrO_3, which is quite appropriate for the enthalpy of the migration of Frenkel defects (Table 2). As evident from Table 2, activation energy (h_m) is less than the heat of transport (Q). In view of this fact, Paddle wheel mechanism is the only mechanism which can suitably be used to explain the transport mechanism of K_2ZrO_3 solid in its superionic phase.

In most of the superionic solids, mobile ions are disordered in the superionic phase. There exists a large number of equal energy sites in the lattice as compared to the number of mobile ions. Due to this reason, ion conduction becomes fast and mobility of ions becomes extremely high. Further, an ion resides on a well-defined lattice site for an average time t_R, then it jumps to another site by crossing a potential barrier in a flight time t_F, where $t_F << t_R$. In some superionic solids, t_F is comparable to t_R, hence the motion between sites becomes important. The oscillation in the potential well should also be taken into account. The effect of lattice vibrations on the mobile ions appears as a friction and a random force which accounts for lattice distortion, is carried on with the particles as they move with it. Hence coupling exists between the moving particles and the rigid frame work. The ZrO^{-2} ions form the rigid lattice and K^+ ions are the mobile ions in K_2ZrO_3 samples. During the electrical transport in K_2ZrO_3, the rotational disorderness of the ZrO^{-2} ions causes strong effect on the mobility of K^+ ions which is considerably enhanced. This mechanism is termed as Paddle Wheel Mechanism and the model is called Cog Wheel Model. A strong coupling between the rotation of the zirconate ion and the K' ion diffusion takes place in case of K_2ZrO_3 while other ion groups remain stationary. Translational motion of cations is strongly enhanced by the rotational

disorderness of the translationary static anions. Therefore, Paddle Wheel mechanism unambiguously suits here for understanding the rotator phase with cation movement in K_2ZrO_3 superionic solid [12-16].

6. CONCLUSION

The solid electrolytes prepared namely; potassium zirconate possess monoclinic unit cell. The phase transition temperature (T_p) of K_2ZrO_3 is observed at 980 K. Below T_p, the compound behaves like a normal ionic conductor in which the electrical conductivity is predominantly due to ions with electronic conduction up to 2 to 7% in 1 to 5% in of K_2ZrO_3. Above T_p, the superionic phase of the compound has been observed in which electrical conductivity is almost ionic in nature with negligible electronic conductivity (≈0.16% in K_2ZrO_3). Frenkel defects are solely responsible for the electrical conductivity. Further, Paddel Wheel Mechanism can be used to explain the ion transport mechanism in K_2ZrO_3 compound.

REFERENCES

[1] S. Chandra; “Superionic Solids: Principles and Applications”, Amsterdam: North-Holland, 1981.

[2] P.G. Bruce (*ed.*); “Solid State Electrochemistry”, No. 5, Combridge University Press, New York, 1995.

[3] P.P. Kumar and S. Yashonath; “Ionic conduction in the solid state”, J Chem. Sci., Vol. 118, pp. 135-154, 2006.

[4] R.C. Agrawal and R.K. Gupta; “Superionic solid: composite electrolyte phase – an overview”, J. Mater. Sci., Vol.34, pp.1131-1162,1999.

[5] N. Kamaya, K. Homma, Y. Yamakawa, M. Hirayama, R. Kanno, M. Yonemura, T. Kamiyama, Y. Kato, S. Hama, K. Kawamoto and A. Mitsui; “A lithium superionic conductor”, Nature Materials, Vol.10, pp. 682–686, 2011.

[6] S.A. Suthanthiraraj and V. Methew; “AC Conductivity, XRD and Transport Properties of Melt Quenched Pb- I_2-Ag_2O-Cr_2O_3 System”, Ionics, Vol.14, pp. 79-83, 2008.

[7] K. Padmasree and D.K. Kanchan; “Conductivity and Di- electric Studies on $20CdI_2$-$80[xAg_2O$-$y(0.7V_2O_5$-$0.3B_2O_3)]$ Super Ion Conducting System”, J. Non-Cryst. Solids, Vol. 352, pp. 3841-3848, 2006.

[8] M. Pant, D.K. Kanchan, P. Sharma and M. Jayswal; “Mixed Conductivity Studies in Silver Oxide Based Barium Vanado-Tellurite Glasses”, Science and Engineering B, Vol. 149, pp. 18-25, 2008.

[9] H.B. Lal, K. Gaur and A.J. Pathak; "Electrical transport in the system Li_2SO_4-mLi_2MoO_4-$2mLi_3VO_4J$", Mater. Sci., Vol. 25, pp. 3683-3687, 1990.

[10] K. Shahi; "Transport studies on superionic conductors", Physica status solidi (a), Vol. 41 (1), pp. 11-44, 1977.

[11] B.K. Verma and H.B. Lal; "Electrical transport studies on heavy rare-earth tungstates", Mater. Res. Bull., Vol.16, pp. 1579-1591, 1981.

[12] K.M. Mishra, A.K. Lal and F.Z. Haque; "Ionic and electronic conductivity in some alkali vanadates", Solid State Ionics, Vol.167, pp. 137-146, 2004.

[13] K. Gaur, A.J. Pathak and H.B. Lal; "Electrical conduction in lithium molybdates", J. Mater. Sci., Vol.5, pp. 785–786, 1986.

[14] K. Gaur, A.J. Pathak and H.B. Lal; "Some new data on lithium sulphate", J. Mater. Sci. Lett., Vol. 7, pp. 425–427, 1988.

[15] S. Tripathi, K.M. Mishra and S.N. Tiwari; "Electrical conduction of superionic conductors: Na_2ZrO_3", Emerg. Mater. Res. USA, Vol. 1(4), pp. 205–211, 2012.

[16] S. Tripathi, K.M. Mishra and S.N. Tiwari; "Mass and Charge Transport in Na_3AsO_4", J. Sci. Tech. Res., Vol. 1, pp. 70-74, 2011.